

An optimized Schwarz method with two-sided Robin transmission conditions for the Helmholtz equation

M. J. Gander¹, L. Halpern² and F. Magoulès^{3,*},[†]

¹*Section de Mathématiques, 2-4 rue du Lièvre, CP 64 CH-1211 Genève, Switzerland*

²*LAGA, Université Paris 13, 93430 Villetaneuse, France*

³*Applied Mathematics and Systems Laboratory, Ecole Centrale Paris, Grande Voie des Vignes, 92295 Châtenay-Malabry Cedex, France*

SUMMARY

Optimized Schwarz methods are working like classical Schwarz methods, but they are exchanging physically more valuable information between subdomains and hence have better convergence behaviour. The new transmission conditions include also derivative information, not just function values, and optimized Schwarz methods can be used without overlap. In this paper, we present a new optimized Schwarz method without overlap in the 2d case, which uses a different Robin condition for neighbouring subdomains at their common interface, and which we call two-sided Robin condition. We optimize the parameters in the Robin conditions and show that for a fixed frequency ω , an asymptotic convergence factor of $1 - O(h^{1/4})$ in the mesh parameter h can be achieved. If the frequency is related to the mesh parameter h , $h = O(1/\omega^\gamma)$ for $\gamma \geq 1$, then the optimized asymptotic convergence factor is $1 - O(\omega^{(1-2\gamma)/8})$. We illustrate our analysis with 2d numerical experiments. Copyright © 2007 John Wiley & Sons, Ltd.

Received 13 March 2006; Revised 8 November 2006; Accepted 10 November 2006

KEY WORDS: Schwarz; domain decomposition; transmission conditions; Helmholtz equation; acoustics

1. INTRODUCTION

The classical Schwarz algorithm was invented by Schwarz more than a century ago [1] to prove existence and uniqueness of solutions to Laplace's equation on irregular domains. The convergence properties of the classical Schwarz methods are well understood, see, for example, the books [2–5]. Over the last 15 years, people have looked at different transmission conditions for the classical Schwarz method, since without overlap the method does not converge. Robin conditions with a

*Correspondence to: F. Magoulès, Applied Mathematics and Systems Laboratory, Ecole Centrale Paris, Grande Voie des Vignes, 92295 Châtenay-Malabry Cedex, France.

[†]E-mail: frederic.magoules@hotmail.com

real parameter have been proposed in [6] to obtain a convergent algorithm for a positive definite model problem. For Helmholtz problems, Robin conditions with a complex parameter were first proposed and analysed in [7], and later in [8–13]. The name optimized Schwarz methods was introduced in [14] to denote the class of Schwarz methods with improved transmission conditions that has been developed over the previous years in [15–17]; for an up to date historical review, and complete results for the positive definite case, see [18]. For Helmholtz problems, optimized Schwarz methods were studied and analysed with one-sided Robin transmission conditions, and second order transmission conditions in [19–21]. A different approach using perfectly matched layers was proposed in [22]. In this paper, we relax the constraint that from both sides on the interface the same Robin condition has to be used, as done in [18] for positive definite problems and in [23] for heterogeneous media. This leads to a new zeroth order optimized Schwarz method with enhanced performance for the Helmholtz equation. We find that the new algorithm has for fixed frequency parameter ω an asymptotic convergence factor of $1 - O(h^{1/4})$ in the mesh parameter h , in contrast to earlier optimized zeroth order Schwarz methods with a performance of $1 - O(h^{1/2})$, see [19]. The new factor is as good as the best factors obtained so far with second order optimized Schwarz methods [24]. If the frequency is related to the mesh parameter h , $h = O(1/\omega^\gamma)$ for $\gamma \geq 1$, then the optimized asymptotic convergence factor is $1 - O(\omega^{(1-2\gamma)/8})$. We illustrate our analysis by 2d numerical examples on a model problem and a large-scale problem.

2. PROBLEM DESCRIPTION AND GENERAL RESULTS

We study in this paper an optimized Schwarz method for the Helmholtz equation

$$\mathcal{L}u := (-\omega^2 - \Delta)u = f \quad \text{in } \Omega \tag{1}$$

where Ω is a bounded domain in two dimensions, and ω is a strictly positive real number. As a model problem we consider the geometry given in Figure 1 on the left. We impose Dirichlet boundary conditions on the horizontal boundaries, and Robin boundary conditions on the vertical boundaries

$$u = 0 \quad \text{on } \tilde{\Gamma}_j, \quad (\partial_{n_j} + s_j)u = g_j \quad \text{on } \Gamma_j, \quad j = 1, 2 \tag{2}$$

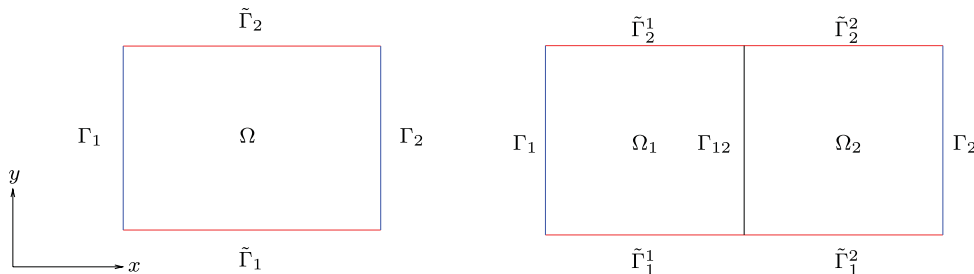


Figure 1. Geometry of the global domain Ω on the left, and decomposition of the domain Ω into two non-overlapping subdomains Ω_1 and Ω_2 on the right.

Here n_j is the unit outward normal to the boundary and s_j is a complex number. We first define the weak solution of (1) and (2). Let $\|\cdot\|$ be the norm in $L^2(\Omega)$ and let $V(\Omega)$ be the space of functions in $H^1(\Omega)$ such that the traces on $\tilde{\Gamma}_j$ vanish. Since the Poincaré inequality holds in this case (see [25]), V can be equipped with the norm $\|v\|_{V(\Omega)} = \|\nabla v\|$. We define in $V(\Omega)$ the sesquilinear form

$$a(u, v) = \int_{\Omega} \nabla u \cdot \nabla \bar{v} \, dx \, dy - \omega^2 \int_{\Omega} u \bar{v} \, dx \, dy + \sum_{j=1}^2 s_j \int_{\tilde{\Gamma}_j} u \bar{v} \, dy \quad (3)$$

and the antilinear form

$$l(v) = \int_{\Omega} f \bar{v} \, dx \, dy + \sum_{j=1}^2 \int_{\Gamma_j} g_j \bar{v} \, dy \quad (4)$$

The weak formulation of problem (1), (2) is to find u in $V(\Omega)$ such that

$$a(u, v) = l(v) \quad \forall v \in V(\Omega) \quad (5)$$

Theorem 2.1

Suppose f is in $V(\Omega)'$ and g_j is in $L^2(\Gamma_j)$. If $\text{Im } s_1 \times \text{Im } s_2 > 0$, then problem (5) has a unique solution u in $V(\Omega)$, which is also solution of the strong form of (5)

$$\begin{aligned} -\omega^2 u - \Delta u &= f && \text{in } \Omega \\ u &= 0 && \text{on } \tilde{\Gamma}_j \\ (\partial_{n_j} + s_j)u &= g_j && \text{on } \Gamma_j \end{aligned} \quad (6)$$

Proof

The proof uses the Fredholm alternative and can be found in [12]. \square

In order to define our algorithm, we need more regularity. We define $\tilde{H}^s(\Gamma_j)$ to be the space of all g defined on Γ_j such that the extension of g by 0 outside Γ_j is in $H^s(\mathbb{R})$.

Theorem 2.2

If f is in $L^2(\Omega)$ and g_j is in $\tilde{H}^{1/2}(\Gamma_j)$, then the variational solution u is in $H^{2-\varepsilon}(\Omega)$ for any positive ε .

Proof

To prove this result, we compute the solution explicitly in the vicinity of a corner and analyse its singularity. The complete proof will appear in [26]. \square

3. DEFINITION AND CONVERGENCE OF THE ALGORITHM

We decompose the domain Ω into two non-overlapping subdomains Ω_1 and Ω_2 , as illustrated in Figure 1 on the right, and consider an optimized Schwarz method with Robin transmission

conditions

$$\begin{aligned}
 -\omega^2 u_1^n - \Delta u_1^n &= f & \text{in } \Omega_1, & & -\omega^2 u_2^n - \Delta u_2^n &= f & \text{in } \Omega_2 \\
 u_1^n &= 0 & \text{on } \tilde{\Gamma}_j^1, & \quad j = 1, 2, & u_2^n &= 0 & \text{on } \tilde{\Gamma}_j^2, & \quad j = 1, 2 \\
 (\partial_{n_1} + s_1)u_1^n &= 0 & \text{on } \Gamma_1, & & (\partial_{n_2} + s_2)u_2^n &= 0 & \text{on } \Gamma_2 \\
 (\partial_{n_1} + s_{12})u_1^n &= (\partial_{n_1} + s_{12})u_2^{n-1} & \text{on } \Gamma_{12}, & & (\partial_{n_2} + s_{21})u_2^n &= (\partial_{n_2} + s_{21})u_1^{n-1} & \text{on } \Gamma_{12}
 \end{aligned} \tag{7}$$

Here, ∂_{n_j} denotes the outward normal derivative in Ω_j , for $j = 1, 2$. The parameters s_j are complex numbers and correspond to approximations of the radiation condition, of the form $-i\omega + a_j$, $a_j > 0$, see [27]. The other parameters s_{12} and s_{21} will be used to optimize the performance of the algorithm. In view of Theorem 2.1, we assume that $\text{Im} s_{ij} < 0$. Suppose we are given h_j^0 in $\tilde{H}^{1/2}(\Gamma_{12})$. We initialize the algorithm at step 0 by

$$\begin{aligned}
 -\omega^2 u_1^0 - \Delta u_1^0 &= f & \text{in } \Omega_1, & & -\omega^2 u_2^0 - \Delta u_2^0 &= f & \text{in } \Omega_2 \\
 u_1^0 &= 0 & \text{on } \tilde{\Gamma}_j^1, & \quad j = 1, 2, & u_2^0 &= 0 & \text{on } \tilde{\Gamma}_j^2, & \quad j = 1, 2 \\
 (\partial_{n_1} + s_1)u_1^0 &= 0 & \text{on } \Gamma_1, & & (\partial_{n_2} + s_2)u_2^0 &= 0 & \text{on } \Gamma_2 \\
 (\partial_{n_1} + s_{12})u_1^0 &= h_1^0 & \text{on } \Gamma_{12}, & & (\partial_{n_2} + s_{21})u_2^0 &= h_2^0 & \text{on } \Gamma_{12}
 \end{aligned} \tag{8}$$

By Theorems 2.1 and 2.2, the initialization (8) defines $\{u_1^0, u_2^0\}$ in $\prod_{j=1}^2 V(\Omega_j) \cap H^{2-\varepsilon}(\Omega_j)$. This in turn gives $h_j^1 = (\partial_{n_j} + s_{ji})u_i^0$ in $\tilde{H}^{1/2}(\Gamma_{12})$ and permits to define the algorithm with u_j^n in $V(\Omega_j) \cap H^{2-\varepsilon}(\Omega_j)$, and $(\partial_{n_j} + s_{ji})u_i^n$ in $\tilde{H}^{1/2}(\Gamma_{12})$.

To analyse the dependence of the algorithm on the parameters in the transmission conditions, we consider now the Helmholtz equation (1) in the domain $\Omega = \mathbb{R} \times (0, L)$ with Sommerfeld radiation conditions at infinity, $\lim_{x \rightarrow \pm\infty} \sqrt{|x|}(x/|x| \partial_x u - i\omega u) = 0$. We decompose the domain into two non-overlapping subdomains $\Omega_1 = (-\infty, 0) \times (0, L)$ and $\Omega_2 = (0, \infty) \times (0, L)$. For the analysis it suffices to consider by linearity the case $f = 0$ and to analyse convergence to the zero solution. Expanding in a Fourier series in the y direction

$$u_j^n(x, y) = \sum_{l=1}^{\infty} \hat{u}_j^n(x, l) \sin(k_l y), \quad k_l = \frac{l\pi}{L} \tag{9}$$

we obtain for $l \geq 1$ the Fourier transformed algorithm

$$\begin{aligned}
 (\omega^2 - k_l^2)\hat{u}_1^n + \partial_{xx}^2 \hat{u}_1^n &= 0, & x < 0 \\
 (\partial_x + s_{12})\hat{u}_1^n &= (\partial_x + s_{12})\hat{u}_2^{n-1}, & x = 0 \\
 (\omega^2 - k_l^2)\hat{u}_2^n + \partial_{xx}^2 \hat{u}_2^n &= 0, & x > 0 \\
 (-\partial_x + s_{21})\hat{u}_2^n &= (-\partial_x + s_{21})\hat{u}_1^n, & x = 0
 \end{aligned} \tag{10}$$

We denote by $\lambda(k)$ the root of the characteristic equation $\lambda^2 + (\omega^2 - k^2) = 0$ defined by $\lambda(k) = \sqrt{k^2 - \omega^2}$ for $|k| \geq \omega$, and $\lambda(k) = -i\sqrt{\omega^2 - k^2}$ for $k < \omega$. Since the Sommerfeld radiation condition excludes growing solutions as well as incoming modes at infinity we obtain the solutions

$\hat{u}_1^n(x, l) = \hat{u}_1^n(0, l)e^{\lambda(k_l)x}$ and $\hat{u}_2^n(x, l) = \hat{u}_2^n(0, k_l)e^{-\lambda(k_l)x}$. Using the transmission conditions and the fact that $\partial_{n_j}\hat{u}_j^n = \lambda(k_l)\hat{u}_j^n$, we obtain over one step of the Schwarz iteration

$$\hat{u}_1^n(x, l) = \frac{s_{12} - \lambda(k_l)}{s_{12} + \lambda(k_l)} e^{\lambda(k_l)x} \hat{u}_2^{n-1}(0, l) \quad \text{and} \quad \hat{u}_2^n(x, l) = \frac{s_{21} - \lambda(k_l)}{s_{21} + \lambda(k_l)} e^{-\lambda(k_l)x} \hat{u}_1^{n-1}(0, l)$$

Evaluating the second equation of the algorithm at $x=0$ for iteration index n and inserting it into the first equation, we get after evaluating again at $x=0$, $\hat{u}_1^n(0, l) = \rho(k_l)\hat{u}_1^{n-2}(0, l)$, where the convergence factor ρ is defined by

$$\rho(k) = \frac{s_{12} - \lambda(k)}{s_{12} + \lambda(k)} \cdot \frac{s_{21} - \lambda(k)}{s_{21} + \lambda(k)} \quad (11)$$

Setting the two complex parameters $s_{12} = p_1 - iq_1$ and $s_{21} = p_2 - iq_2$, with p_j and q_j in \mathbb{R} , and inserting s_{12} and s_{21} into the convergence factor (11), we find after simplifying

$$|\rho(p_1, q_1, p_2, q_2, k)|^2 = \begin{cases} \frac{p_1^2 + (q_1 - \sqrt{\omega^2 - k^2})^2}{p_1^2 + (q_1 + \sqrt{\omega^2 - k^2})^2} \frac{p_2^2 + (q_2 - \sqrt{\omega^2 - k^2})^2}{p_2^2 + (q_2 + \sqrt{\omega^2 - k^2})^2}, & k^2 < \omega^2 \\ \frac{q_1^2 + (p_1 - \sqrt{k^2 - \omega^2})^2}{q_1^2 + (p_1 + \sqrt{k^2 - \omega^2})^2} \frac{q_2^2 + (p_2 - \sqrt{k^2 - \omega^2})^2}{q_2^2 + (p_2 + \sqrt{k^2 - \omega^2})^2}, & k^2 \geq \omega^2 \end{cases} \quad (12)$$

Theorem 3.1

For any $p_j, q_j > 0$, and any $\omega > 0$ such that $\omega \neq k_l, l \in \mathbb{N}^+$, the convergence factor $\rho(k_l)$ is strictly less than one in modulus and the algorithm converges in $\prod L^2(\Omega_j)$.

Proof

With the assumptions on the coefficients, (12) shows that $|\rho(p_1, q_1, p_2, q_2, k_l)| < 1$ for $k_l \neq \omega$. By induction, $\hat{u}_j^{2n}(x, l) = \rho^{2n}\hat{u}_j^0(x, l)$, and to show convergence in $\prod L^2(\Omega_j)$, we compute the L^2 -norm

$$\|u_j^{2n}\|^2 = \frac{1}{2} \sum_{l=1}^{\infty} \|\hat{u}_j^{2n}(\cdot, l)\|_{L^2(\mathbb{R}_-)}^2 = \frac{1}{2} \sum_{l=1}^{\infty} |\rho(k_l)|^{2n} \|\hat{u}_j^0(\cdot, l)\|_{L^2(\mathbb{R}_-)}^2$$

If the initial guess u_j^0 is in L^2 , the series with general term $\|\hat{u}_j^0(\cdot, l)\|^2$ converges, and $|\rho(k_l)|^{2n}$ tends to zero as $n \rightarrow \infty$. So by Lebesgue's Theorem, u_j^{2n} tends to zero in $L^2(\Omega_j)$. The same holds for odd iterates. \square

4. OPTIMIZATION OF THE TRANSMISSION CONDITIONS

We want to determine the two complex parameters $s_{12} = p_1 - iq_1$, and $s_{21} = p_2 - iq_2$ to get the best performance of algorithm (7). Previous optimized Schwarz methods with Robin transmission conditions reduced the number of free parameters by setting $s_{12} = s_{21}$. This led in [19–21] to an optimized Schwarz method with asymptotic convergence factor $\rho = 1 - O(h^{1/2})$, where h denotes the mesh parameter. Here, we do not make this simplifying assumption, and we say that the algorithm is using two-sided Robin transmission conditions. This leads to an algorithm which is more efficient both initially and asymptotically than the earlier one with one-sided Robin

transmission conditions. To find the best choice for s_{12} and s_{21} , without knowing which frequencies k_l will be present in the errors in the transformed optimized Schwarz method (10), the idea is to minimize $|\rho(k_l)|^2$ in (12) for all k_l that could be present in the iteration. From the Fourier series (9), we see that the lowest frequency is $k_{\min} := k_1 = \pi/L$. Now for the continuous problem, the highest frequency would be $k_\infty = \infty$, but in a discretization with mesh parameter h , the largest frequency supported by the numerical grid is $k_{\max} = C/h$, where the constant C can be estimated by $C = \pi$, since the highest possible oscillation on a grid with spacing h is to oscillate between the values 1 and -1 at each node. It suffices therefore to minimize $|\rho(k_l)|^2$ for integers l such that $k_l \in [k_{\min}, k_{\max}]$. We approximate here the minimization on the discrete spectrum by the minimization on two continuous intervals

$$\min_{p_j, q_j \in \mathbb{R}} \left(\max_{k \in (k_{\min}, k_-) \cup (k_+, k_{\max})} |\rho(p_1, q_1, p_2, q_2, k)|^2 \right) \tag{13}$$

where $k_- = \lfloor \omega L / \pi \rfloor \pi / L$ and $k_+ = \lceil \omega L / \pi \rceil \pi / L$. As we have seen in Theorem 3.1, we need $\omega \neq k$ for convergence, since for $k = \omega$, the convergence factor $\rho(p_1, q_1, p_2, q_2, k) = 1$, independently of what one chooses for the parameters p_j and q_j . The frequency $k = \omega$ represents, however, only one single mode in the spectrum, and a Krylov method will easily take care of this when the Schwarz method is used as a preconditioner. We therefore choose in that case $k_- = \omega - \pi/L$ and $k_+ = \omega + \pi/L$, and still optimize by solving (13).

The complete study of the best approximation problem (13) is beyond the scope of this short paper and will appear in [26]. By an asymptotic analysis of (13), we obtain, however, the following result:

Theorem 4.1

Let ω be fixed, and let $k_{\min} < k_- < \omega < k_+ < k_{\max} = C/h$. Then for h small, the parameters

$$p_1 = q_1 = \frac{C^{3/4} C_\omega^{1/8}}{h^{3/4}}, \quad p_2 = q_2 = \frac{C^{1/4} C_\omega^{3/8}}{2h^{1/4}} \tag{14}$$

lead to the asymptotic convergence factor

$$\max_{k \in (k_{\min}, k_-) \cup (k_+, k_{\max})} |\rho(p_1, q_1, p_2, q_2, k)|^2 = 1 - \frac{4C_\omega^{1/8}}{C^{1/4}} h^{1/4} + O(h^{1/2}) \tag{15}$$

where $C_\omega = \omega^2 - k_-^2$ if $2\omega^2 \leq k_-^2 + k_+^2$, and $C_\omega = k_+^2 - \omega^2$ otherwise.

Proof

It suffices to insert the parameter choice (14) into the modulus of the convergence factor $\rho(p_1, q_1, p_2, q_2, k)$ in (12), to expand for h small, and to verify. □

In practice however, other limits are of interest as well. A rule of thumb says that one needs about 10 points per wavelength resolution, which means that the mesh parameter h is coupled with the frequency of the problem ω , through the relation $h = C_h/\omega = \pi/5\omega$. Furthermore, it has been shown in [28] that for an accurate discretization when ω becomes large, one even needs more points per wavelength, namely $h = C_h/\omega^\gamma$, $\gamma > 1$. Here, γ depends on the discretization, for example, $\gamma = 3/2$ for a \mathbb{P}_1 finite element method.

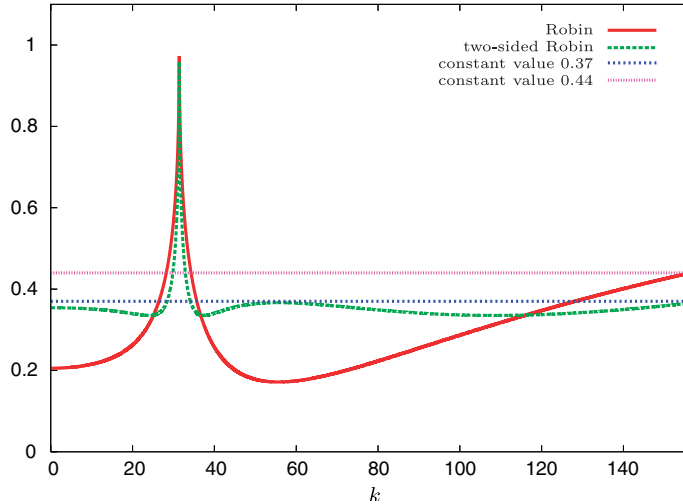


Figure 2. Convergence factor of the optimized Schwarz method with the one-sided optimized Robin conditions and the new two-sided optimized Robin conditions as a function of the Fourier parameter k , for $\omega = 10\pi$ and $h = \frac{1}{50}$.

Theorem 4.2

Let $k_- = \omega - \delta k_-$, $k_+ = \omega + \delta k_+$, and let $h = C_h/\omega^\gamma$. If $\gamma = 1$ and $\pi > \sqrt{2}C_h$, then for ω large, the parameters

$$p_1 = q_1 = (2\delta k)^{1/8} \frac{(C^2 - C_h^2)^{3/8}}{C^{3/4}} \omega^{7/8}, \quad p_2 = q_2 = (2\delta k)^{3/8} \frac{(C^2 - C_h^2)^{1/8}}{2C^{1/4}} \omega^{5/8} \quad (16)$$

lead to the asymptotic convergence factor

$$\max_{k \in (k_{\min}, k_-) \cup (k_+, k_{\max})} |\rho(p_1, q_1, p_2, q_2, k)|^2 = 1 - 4(2\delta k)^{1/8} \frac{C_h^{1/4}}{(C^2 - C_h^2)^{1/8}} \omega^{-1/8} + O(\omega^{-1/4}) \quad (17)$$

where $\delta k = \max(\delta k_+, \delta k_-)$. If $\gamma > 1$, then for ω large, the parameters

$$p_1 = q_1 = (2\delta k)^{1/8} \frac{C^{3/4}}{C_h^{3/4}} \omega^{(6\gamma+1)/8}, \quad p_2 = q_2 = (2\delta k)^{3/8} \frac{C^{1/4}}{2C_h^{1/4}} \omega^{(2\gamma+3)/8} \quad (18)$$

lead to the asymptotic convergence factor

$$\max_{k \in (k_{\min}, k_-) \cup (k_+, k_{\max})} |\rho(p_1, q_1, p_2, q_2, k)|^2 = 1 - 4(2\delta k)^{1/8} \frac{C_h^{1/4}}{C^{1/4}} \omega^{(1-2\gamma)/8} + o(\omega^{(1-2\gamma)/8}) \quad (19)$$

Proof

Again, it suffices to insert the parameter choice (16) and (18), respectively, into the modulus of the convergence factor $\rho(p_1, q_1, p_2, q_2, k)$ in (12), to expand for ω large, and to verify. \square

Note that the condition $\pi > \sqrt{2}C_h$ in the first part of Theorem 4.2 is not restrictive, since the minimum requirement of 10 points per wavelength leads to $C_h = \pi/5$, and thus the condition is satisfied.

Figure 2 shows the convergence factor obtained for a model problem on the unit square with two subdomains, $\omega = 10\pi$ and $h = \frac{1}{50}$. The optimal parameter for the old one-sided optimized Robin condition was found to be $s_1 = s_2 = 32.462(1 - i)$, which gives an overall convergence factor of $\rho = 0.4416$, whereas for the two-sided Robin condition the parameters are $s_1 = 86.874(1 - i)$ and $s_2 = 12.130(1 - i)$, which gives an overall convergence factor of $\rho = 0.3664$, which means 20% less iterations, at the same cost per iteration.

5. NUMERICAL EXPERIMENTS

5.1. A model problem

We show first numerical experiments on a model problem which correspond to our analysis with two-subdomains only. We study a two-dimensional cavity on the unit square Ω with homogeneous Dirichlet conditions on top and bottom, and on the left and right radiation conditions of Robin type. We decompose the unit square into two subdomains of equal size and we use a uniform rectangular mesh for the discretization. We perform all our experiments directly on the error equations, $f = 0$, and choose the initial guess of the Schwarz iteration so that all the frequencies are present in the error. We show two sets of experiments: the first one uses $\omega = 9.5\pi$, thus excluding ω from the frequencies k_l relevant in this setting, $k_l = l\pi$, $l = 1, 2, \dots$. This allows us to test directly the iterative Schwarz method, since with optimization parameters $k_- = 9\pi$ and $k_+ = 10\pi$ we obtain a convergence factor which is uniformly less than one for all k_l , $l = 1, 2, \dots$.

Table I shows the number of iterations needed for different values of the mesh parameter h for one-sided optimized Robin conditions (see [19, 20]), and the new two-sided optimized Robin conditions (see Theorem 4.1), and compares the results with Taylor conditions (i.e. $s_{12} = s_{21} = i\omega$, see [7]) in the case of Krylov acceleration (without, Taylor conditions do not lead to a convergent algorithm, because for all frequencies $k > \omega$, the convergence factor equals 1). The Krylov method used in this section is GMRES. Note that the two-sided optimized Robin condition decreases the number of iterations by almost a factor of 2 over the one-sided optimized Robin transmission

Table I. Number of iterations when ω does not lie on a frequency of the problem.

h	Iterative		Krylov		
	Optimized	Two-sided optimized	Taylor	Optimized	Two-sided optimized
$\frac{1}{50}$	457	322	26	16	14
$\frac{1}{100}$	126	70	34	21	17
$\frac{1}{200}$	153	75	44	26	20
$\frac{1}{400}$	215	91	57	34	23
$\frac{1}{800}$	308	112	72	43	27

condition at $h = \frac{1}{100}$ and by almost a factor of 3 at $h = \frac{1}{800}$, at the same cost per iteration. When Krylov acceleration is used, one still gains a factor of about 1.6.

Figure 3 shows the asymptotic behaviour of the methods considered. The asymptotic analysis is confirmed for the iterative version of the optimized methods. In addition one can see that the Krylov method improves the asymptotic factor, but a bit less than an additional square root. Note the outlier for $h = \frac{1}{50}$, which is due to the discrepancy between the spectrum of the continuous and the discrete operator: $\omega = 9.5\pi$ lies precisely in between two frequencies 9π and 10π at the continuous level, but for the discrete Laplacian with $h = \frac{1}{50}$ this spectrum is shifted to 8.88π and 9.84π and thus the frequency 9.84π falls into the range $[9\pi, 10\pi]$ neglected by the optimization. Note, however, that this is of no importance when Krylov acceleration is used, so it is not worthwhile to consider this issue further.

Now we put ω directly onto a frequency of the model problem, $\omega = 10\pi$, so that the iterative methods cannot be considered any more, since for that frequency the convergence factor equals 1. The Krylov accelerated versions, however, are not affected by this, as one can see in Table II. The number of iterations does not differ from the case where ω was chosen to lie between two frequencies, which shows that with Krylov acceleration the method is robust for any values of ω .

Now we fix $h\omega = \text{const}$ to see how the optimized Schwarz method behaves for higher and higher values of ω , which corresponds to Theorem 4.2. Table III shows the number of iterations as ω is increased, and shows that the method also behaves well in that case.

We finally tested for the smallest resolution of the model problem how well Fourier analysis predicts the optimal parameters to use. Since we want to test both the iterative and the Krylov versions, we need to put again the frequency ω in between two problem frequencies, and in this case it is important to be precise. We therefore choose ω to be exactly between two frequencies of

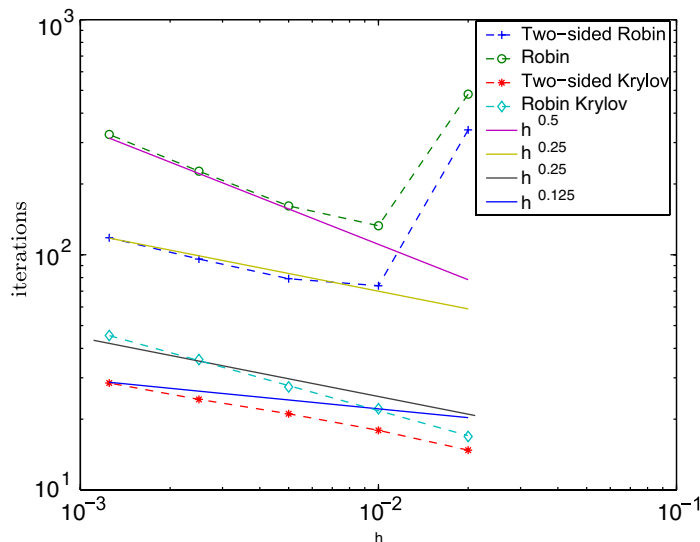


Figure 3. Asymptotic behaviour of the optimized Schwarz method with the one-sided optimized Robin conditions and the new two-sided optimized Robin conditions for $\omega = 10\pi$.

Table II. Number of iterations when ω lies precisely on a frequency of the problem and thus Krylov acceleration is mandatory.

h	Krylov		
	Taylor	Optimized	Two-sided optimized
$\frac{1}{50}$	24	15	13
$\frac{1}{100}$	35	21	17
$\frac{1}{200}$	44	26	20
$\frac{1}{400}$	56	33	23
$\frac{1}{800}$	73	43	27

Table III. Number of iterations when ω increases and $h\omega$ is held constant.

ω	Krylov		
	Taylor	Optimized	Two-sided optimized
10π	24	15	13
20π	33	21	18
40π	43	24	20
80π	53	27	21
160π	83	44	32

the discrete problem, $\omega = 9.3596\pi$, and optimized using $k_- = 8.8806\pi$ and $k_+ = 9.8363\pi$. Figure 4 shows the number of iterations the algorithm needs to achieve a residual of 10^{-6} as a function of the optimization parameters p_1 and p_2 , on the left in the iterative version and on the right for the Krylov accelerated version. The Fourier analysis shows quite well where the optimal parameters lie, and when a Krylov method is used, the optimized Schwarz method is very robust with respect to the choice of the optimization parameters.

5.2. Airplane noise emission

We analyse now the noise level distribution near a city located close to an airport. The main objective of this evaluation is the synthesis of the frequency response function at the buildings as a result of noise generated by the engine of an airplane during the landing procedure. The initial noise can come from various mechanisms (air-borne or structural-borne vibrations) and can be difficult to predict. We perform a two-dimensional simulation on a vertical cross-section of the city, for an A340 airplane of length 63.60 m and height 16.70 m. We impose Dirichlet boundary conditions along the engine of the airplane, homogeneous Neumann boundary conditions on the plane, on the ground and on the buildings, and the Bayliss–Gunzburger–Turkel absorbing condition on the artificial boundary. The imaginary part of the Galerkin solution is shown in Figure 6. Table IV shows the performance of the optimized Schwarz method. Taylor conditions, optimized one-sided Robin conditions and the new two-sided optimized Robin conditions are compared for a series of

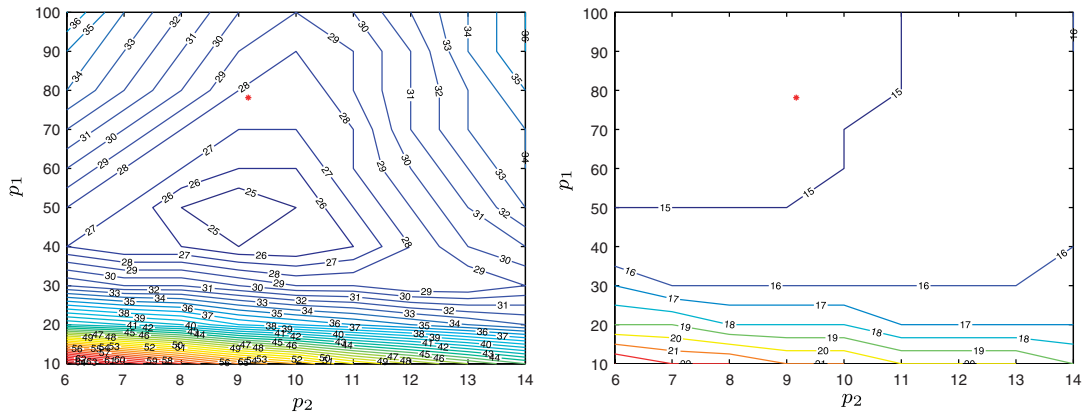


Figure 4. Number of iterations needed to achieve a given precision, as a function of the optimization parameters p_1 and p_2 in the two-sided Robin transmission conditions, on the left for the iterative algorithm and on the right for the Krylov accelerated one. The star denotes the optimized parameters found by our Fourier analysis.

Table IV. Number of iterations when the number of unknowns increases.

Unknowns	Krylov		
	Taylor	Optimized	Optimized 2p
210 296	172	119	58
370 794	183	132	66
576 215	194	147	72

discrete models involving 210 296, 370 794 and 576 215 grid points, respectively. Each mesh is split into 16 subdomains of regular shape as illustrated in Figure 5. The two-sided optimized Schwarz method described in this paper for the case of two subdomains can be extended to the case of many subdomains, as already shown in [17, 19] for one-sided optimized Schwarz methods. Here, the same idea is used in the special case where each subdomain has one and only one neighbouring subdomain. The corner points between the interfaces and the artificial boundary condition do not lead to particular difficulties in the finite element discretization, since the integration is performed along the interface and the coefficients of the elementary matrices are then simply assembled.

The computations are performed in parallel on a network of PCs. The Krylov method used in this section is ORTHODIR. We stop the iteration when the residual reaches 10^{-8} . Table IV clearly shows the efficiency and the robustness of the new optimized Schwarz method with two-sided Robin transmission conditions.

6. CONCLUSIONS

We introduced a new optimized Schwarz method without overlap for Helmholtz problems which uses two-sided Robin transmission conditions, i.e. Robin transmission conditions with different

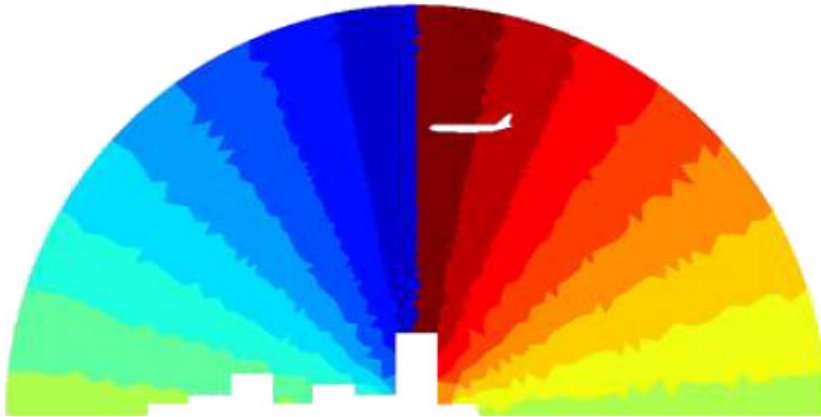


Figure 5. Domain decomposition into 16 subdomains.

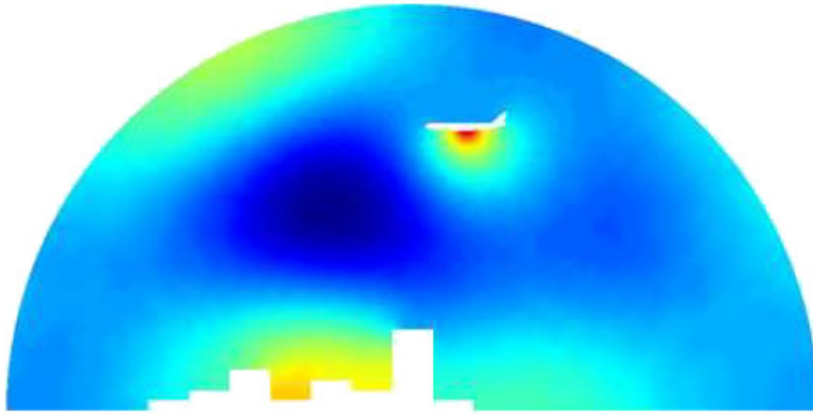


Figure 6. A340 airplane noise emission over the city.

parameters depending on which side of the interface we are on. We analysed a model problem with two subdomains, proved convergence of the algorithm, and showed that the performance of the new optimized Schwarz method is asymptotically better than the performance when the same parameter is used in the Robin transmission conditions. Numerical experiments showed that the method behaves asymptotically as predicted on a model problem, and is very efficient on a large-scale acoustic problem involving more than two subdomains. We are currently extending the ideas presented here to three-dimensional problems.

REFERENCES

1. Schwarz H. Über einen Grenzübergang durch alternierendes Verfahren. *Vierteljahrsschrift der Naturforschenden Gesellschaft in Zürich* 1870; **15**:272–286.
2. Smith B, Björstad P, Gropp W. *Domain Decomposition: Parallel Multilevel Methods for Elliptic Partial Differential Equations*. Cambridge University Press: Cambridge, MA, 1996.

3. Quarteroni A, Valli A. *Domain Decomposition Methods for Partial Differential Equations*. Oxford Science Publications: Oxford, 1999.
4. Toselli A, Widlund O. *Domain Decomposition Methods—Algorithms and Theory*. Springer Series in Computational Mathematics, vol. 34. Springer: Berlin, 2004.
5. Magoulès F, Kako T (eds). *Domain Decomposition Methods: Theory and Applications*. Gakuto International Series, Mathematical Sciences and Applications, vol. 25. Gakkotosho: Tokyo, Japan, 2006.
6. Lions P-L. On the Schwarz alternating method. III: A variant for nonoverlapping subdomains. In *Third International Symposium on Domain Decomposition Methods for Partial Differential Equations*, Chan T, Glowinski R, Périaux J, Widlund O (eds). SIAM: Philadelphia, PA, 1990.
7. Després B. Méthodes de décomposition de domaine pour les problèmes de propagation d'ondes en régimes harmoniques. *Ph.D. Thesis*, Université Dauphine, Paris IX, 1991.
8. Després B. Domain decomposition method and the Helmholtz problem. II. *Second International Conference on Math. and Numer. Aspects of Wave Propagation*. SIAM: Philadelphia, PA, 1993; 197–206.
9. Chevalier P, Nataf F. Symmetrized method with optimized second-order conditions for the Helmholtz equation. *Contemporary Mathematics* 1998; 400–407.
10. de la Bourdonnaye A, Farhat C, Macedo A, Magoulès F, Roux F-X. A non-overlapping domain decomposition method for the exterior Helmholtz problem. *Contemporary Mathematics* 1998; **218**:42–66.
11. Farhat C, Macedo A, Lesoinne M, Roux F-X, Magoulès F, de la Bourdonnaye A. Two-level domain decomposition methods with Lagrange multipliers for the fast iterative solution of acoustic scattering problems. *Computer Methods in Applied Mechanics and Engineering* 2000; **184**(2):213–240.
12. Collino F, Ghanemi S, Joly P. Domain decomposition methods for harmonic wave propagation: a general presentation. *Computer Methods in Applied Mechanics and Engineering* 2000; **2-4**:171–211.
13. Balabane M. A domain decomposition algorithm for the Helmholtz equation. 1: The dissipating case. *Technical Report 2003-01*, LAGA, Université Villetaneuse, Paris 13, 2003.
14. Gander M, Halpern L, Nataf F. Optimized Schwarz methods. *Twelfth International Conference on Domain Decomposition Methods*, Chiba, Japan, 2001; 15–28.
15. Chevalier P. Méthodes numériques pour les tubes hyperfréquences. Résolution par décomposition de domaine. *Ph.D. Thesis*, Université Pierre & Marie Curie, Paris VI, 1998.
16. Japhet C. Méthodes de décomposition de domaine et conditions aux limites artificielles en mécanique des fluides: méthode optimisée d'ordre 2. *Ph.D. Thesis*, Université Paris Nord, Paris XIII, 1998.
17. Magoulès F. Méthodes numériques de décomposition de domaine pour des problèmes de propagation d'ondes. *Ph.D. Thesis*, Université Pierre & Marie Curie, Paris VI, 2000.
18. Gander MJ. Optimized Schwarz methods. *SIAM Journal on Numerical Analysis* 2006; **44**(2):699–731.
19. Gander M, Magoulès F, Nataf F. Optimized Schwarz methods without overlap for the Helmholtz equation. *SIAM Journal on Scientific Computing* 2002; **24**(1):38–60.
20. Magoulès F, Iványi P, Topping B. Non-overlapping Schwarz methods with optimized transmission conditions for the Helmholtz equation. *Computer Methods in Applied Mechanics and Engineering* 2004; **193**(45–47):4797–4818.
21. Magoulès F, Iványi P, Topping B. Convergence analysis of Schwarz methods without overlap for the Helmholtz equation. *Computers and Structures* 2004; **82**:1835–1847.
22. Toselli A. Some results on overlapping Schwarz methods for the Helmholtz equation employing perfectly matched layers. *Technical Report 765*, New York University, Courant Institute, 1998.
23. Maday Y, Magoulès F. Non-overlapping additive Schwarz methods tuned to highly heterogeneous media. *Comptes Rendus de l'Académie des Sciences, Paris, Série I* 2005; **341**(11):701–705.
24. Gander M. Optimized Schwarz methods for Helmholtz problems. *Thirteenth International Conference on Domain Decomposition Methods*, Lyon, France, 2001; 245–252.
25. Grisvard P. *Singularities in Boundary Value Problems*, RMA, vol. 22. Masson: Paris, 1992.
26. Gander M, Halpern L, Magoulès F. Optimal asymptotic performance of an optimized Schwarz method without overlap for the Helmholtz equation. *Technical Report*, Ecole Centrale Paris, France, 2006, in preparation.
27. Bayliss A, Turkel E. Radiation boundary conditions for wave-like equations. *Communications on Pure and Applied Mathematics* 1980; **33**(6):707–725.
28. Babuska I, Sauter S. Is the pollution effect of the FEM avoidable for the Helmholtz equation considering high wave numbers? *SIAM Journal on Numerical Analysis* 1997; **27**:323–352.